ESC European Society of Cardiology

European Heart Journal (2020) **41**, 1286–1297
doi:10.1093/eurheartj/ehz552

CLINICAL REVIEW
Basic Science for the clinician

Invasive left ventricle pressure–volume analysis: overview and practical clinical implications

Marcelo B. Bastos [1], Daniel Burkhoff [2], Jiri Maly[3], Joost Daemen [1], Corstiaan A. den Uil [1,4], Koen Ameloot [1], Mattie Lenzen[1], Felix Mahfoud[5], Felix Zijlstra[1], Jan J. Schreuder[1], and Nicolas M. Van Mieghem[1]*

[1]Department of Cardiology, Thoraxcenter, Erasmus University Medical Centre, Office Nt 645, Dr Molewaterplein 40 3015 GD, Rotterdam, The Netherlands; [2]Cardiovascular Research Foundation, New York, NY, USA; [3]Department of Cardiac and Transplant Surgery, IKEM, Prague, Czech Republic; [4]Department of Intensive Care Medicine, Thoraxcenter, Erasmus University Medical Centre, Rotterdam, The Netherlands; and [5]Department of Internal Medicine III, Cardiology, Angiology, Intensive Care Medicine, Saarland University Hospital, Homburg/Saar, Germany

Received 12 January 2019; revised 22 April 2019; editorial decision 20 June 2019; accepted 7 August 2019; online publish-ahead-of-print 21 August 2019

Ventricular pressure–volume (PV) analysis is the reference method for the study of cardiac mechanics. Advances in calibration algorithms and measuring techniques brought new perspectives for its application in different research and clinical settings. Simultaneous PV measurement in the heart chambers offers unique insights into mechanical cardiac efficiency. Beat to beat invasive PV monitoring can be instrumental in the understanding and management of heart failure, valvular heart disease, and mechanical cardiac support. This review focuses on intra cardiac left ventricular PV analysis principles, interpretation of signals, and potential clinical applications.

Keywords Pressure-volume loop • Left ventricular haemodynamics • Myocardial energetics

Introduction

Otto Frank originally described the cardiac cycle and ventricular properties through the window of the pressure–volume (PV) loop in 1895. Suga and Sagawa introduced methods for real-time measurements in *ex vivo* blood-perfused hearts, which spawned research that culminated in unprecedented understanding of ventricular mechanics and energetics. The introduction of the PV catheter by Baan *et al.* facilitated *in vivo* studies.[1–5]

Recently developed algorithms for simplified calibration, single-beat estimation of end-systolic and end-diastolic pressure–volume relations (ESPVR and EDPVR, respectively) and for the evaluation of intra-ventricular dyssynchrony galvanized the interest in PV analysis in the clinical setting.[4–7] The PV analysis can elucidate pathophysiological mechanisms of heart failure (HF), including HF with preserved ejection fraction (HFpEF), myocardial and valvular heart diseases as well as monitoring the effects of therapeutic interventions.[8–20] As such, PV measurements have the potential for increased adoption in contemporary research and clinical practice. The PV loops can be obtained from all cardiac chambers using similar techniques.[20–24] The reader is referred to the specialized literature for a more holistic understanding. This review focuses on the fundamentals of left ventricular (LV) PV analysis highlighting practical aspects of PV measurements, interpretation of signals and potential applications to clinical practice.

Invasive acquisition of LV pressures and volumes

Clinical PV acquisition is made with a 4–7 F PV catheter, containing 12 equidistant electrodes equally spaced with a solid-state pressure sensor in the middle of the electrode array (Inca, CD Leycom). Placement is trans-aortic or trans-septal with its tip in the LV apex with the most proximal electrode above the aortic or mitral valve respectively (*Figure 1*).

In brief, an electrical current (*I*) between distal and proximal electrodes sets up an electrical field. Since blood is partially conductive, the voltage decreases across each successive pair of electrodes. The

* Corresponding author. Tel: +31(0)107035260, Fax: +31(0)104369154, Email: n.vanmieghem@erasmusmc.nl

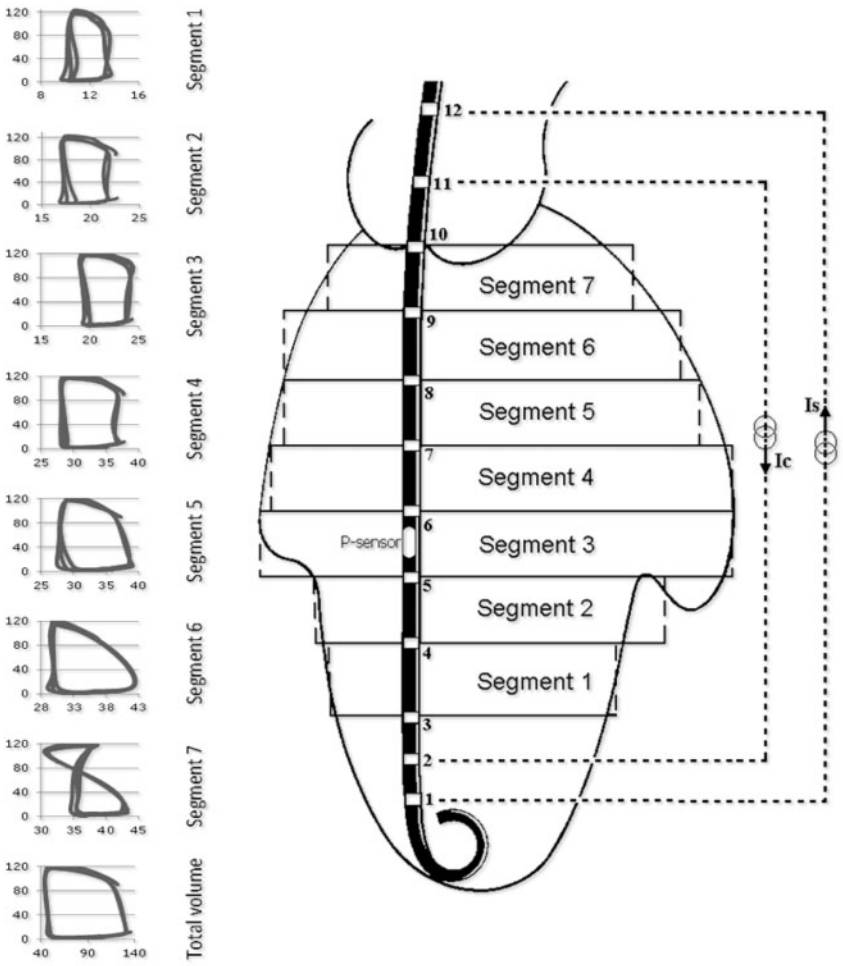

Figure 1 The conductance catheter principle. Ventricular positioning of the pressure–volume catheter with segmental pressure–volume loops from apex (segment 1) to basis (segment 7). Segments 1 to 6 have an upright rectangular shape with time progressing in counter-clockwise manner. In contrast, segment 7 is partially in the aorta with a 'figure-of-8'configuration. Accordingly, the calculation of total volume includes summation only of segments 1 through 6.

voltage drop between two adjacent electrodes (V_i) is inversely related to (i) the cross-sectional area (A_i) of a hypothetical cylindrical segment defined at the level of the electrodes, (ii) the distance between electrodes (D), and (iii) blood resistance (ρ) as measured by the Inca system. The segmental volume between an adjacent pair of electrodes ($Vol_{i,est}$) is estimated by: $Vol_{i,est} \approx A_i \cdot D \approx I \cdot \rho \cdot D^2 / V_i$, where V_i is directly measured. Total LV volume ($V_{total,est}$) is the sum of the volumes of all segments within the LV chamber: $V_{total,est}$ $V_{i,est}$. The number of segments inside the LV is obtained from segmental PV loops as shown in *Figure 1*.[3,4]

The first method of volume calibration relies on immediate pre-procedure measurements of LV end-diastolic volume (V_{ed}) and stroke volume (SV) or ejection fraction (EF) taken from echocardiography, computed tomography, or cardiac magnetic resonance imaging. This concept assumes that chamber dimensions remained constant between the time of imaging acquisition and the time of invasive PV measurement. A second and more accurate method can be drawn from a combination of hypertonic saline infusion into the pulmonary artery or right atrium (to determine 'parallel' conductance) and thermodilution to assess SV.[19]

A few conditions are worth noting. First, volume calibrations must be repeated in case of catheter displacement or haematocrit variations (e.g. in case of bleeding events). If no accurate imaging modality is available the 'hypertonic saline infusion and thermodilution' calibration method should be favoured. Second, pressure calibration is required and needs confirmation to avoid pressure drift between start and end of recording sessions.

Pressure–volume analysis

General considerations

Ideally, the PV loop is rectangular or trapezoidal, depicting the four phases of the cardiac cycle (*Figure 2A*): isovolumetric contraction, ejection, isovolumetric relaxation, and passive filling.

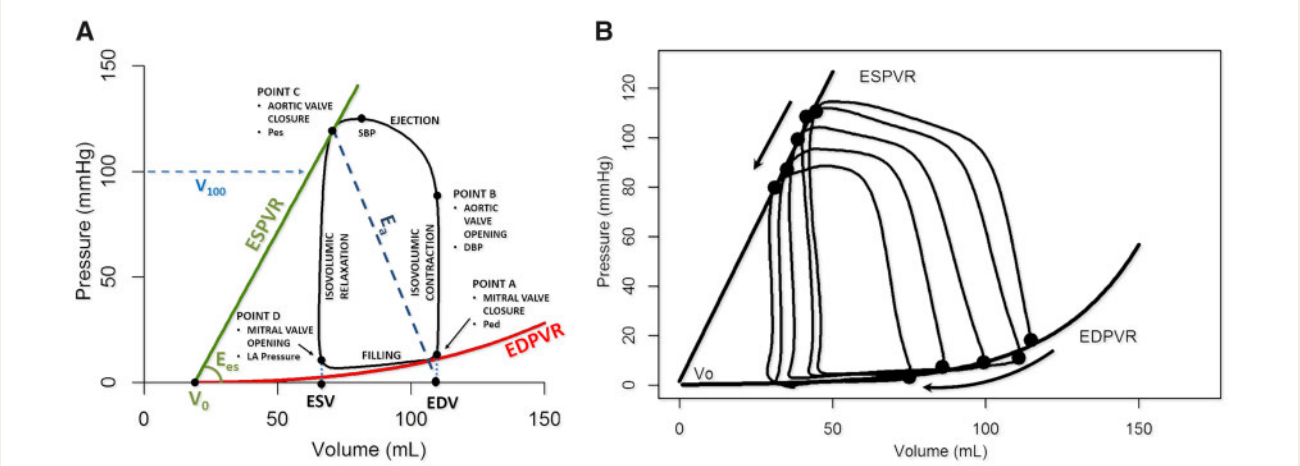

Figure 2 Essential principles of the left ventricular pressure–volume relationship. (*A*) DBP, diastolic blood pressure; E_a, effective arterial elastance; EDPVR, end-diastolic pressure–volume relationship; E_{es}, end-systolic elastance; ESPVR, end-systolic pressure–volume relationship; PE, potential energy; P_{ed}, end-diastolic pressure; P_{es}, end-systolic pressure; SBP, systolic blood pressure; SW, stroke work; V_0, volume at a P_{es} of 0 mmHg. Stroke volume (SV) is EDV - ESV. (*B*) Vena cava occlusion to change/reduce preload (arrow) and determine the end-systolic and end-diastolic relationships by linear regression.

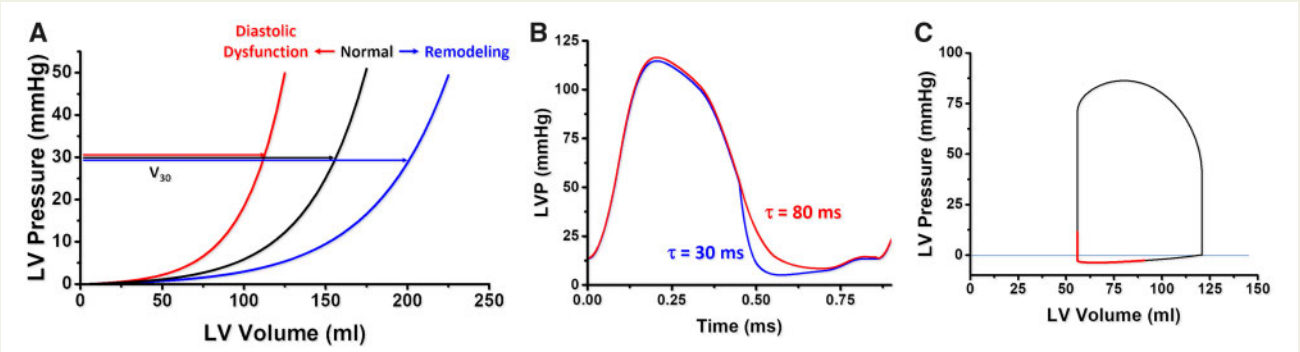

Figure 3 End-diastolic pressure–volume relationship concepts. (*A*) V30 is the left ventricular (LV) volume at a pressure of 30 mmHg and reflects compliance. A shift to the left suggests diastolic dysfunction (red), to the right ventricular remodelling (blue). (*B*) In coronary ischaemia, impaired active relaxation delays the pressure decay (red) increasing τ in early diastole. (*C*) Early diastolic suction in a simulated pressure–volume loop.

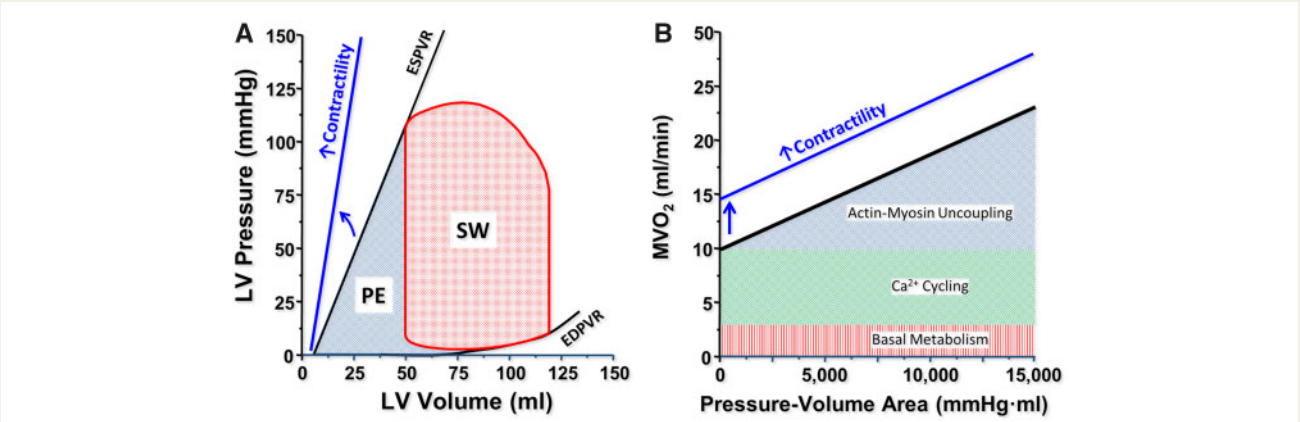

Figure 4 Myocardial energetics. (*A*) The pressure–volume area (PVA) is the sum of stroke work (SW) and potential energy (PE). (*B*) Pressure–volume area correlates linearly with myocardial oxygen consumption per beat. The relation is shifted upwards by increased contractile (e.g. inotropic agents).

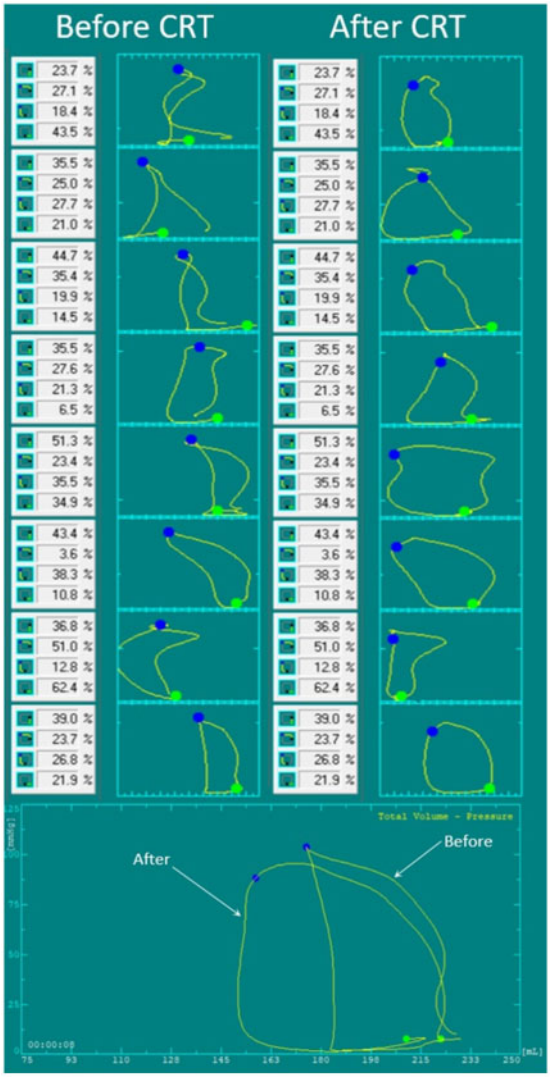

Figure 5 Mechanical dyssynchrony. Segmental and global pressure–volume (PV) loops before and after cardiac resynchronization therapy. Distorted segmental pressure–volume loops out of sync before cardiac resynchronization therapy and more in sync after cardiac resynchronization therapy.

End-systolic and end-diastolic PV relationships (ESPVR and EDPVR) characterize LV systolic and diastolic properties, respectively (each detailed further below). Classically, measurement of these relationships requires transient modulations of preload (e.g. inferior caval vein occlusion) or afterload (e.g. hand grip manoeuvre) (*Figure 2B*).

Single-beat algorithms simplify PV analysis by estimating ESPVRs and EDPVRs from a single steady-state PV loop tracing and further relying on measurements of arterial systolic and diastolic pressures, SV, EF, pre-ejection time period, and total systolic period that are obtained with the conductance catheter, or by non-invasive means using echo-Doppler. These algorithms are readily programmed into spreadsheets and available online.[6,7,18]

Depending on the purpose for which PV loops are measured, single-beat algorithms in combination with simplified means of PV catheter calibration may suffice and thus facilitate PV analysis.

End-systolic pressure–volume relationship

The ESPVR is approximately linear in the physiological range of end-systolic pressures (P_{es}) and volumes (V_{es}) (*Figure 2A*). It is characterized by a slope (end-systolic elastance, E_{es}) and a volume axis intercept V_0 such that $P_{es} = E_{es} \cdot (V_{es} - V_0)$. E_{es} represents the peak chamber elastance during a beat and reflects ventricular chamber mechanical properties when the maximum number of actin-myosin bonds is formed. E_{es} increases with positive inotropism (e.g. *dobutamine, milrinone, levosimendan*) and sympathetic activation, but decreases with negative inotropism (beta-blockers, calcium channel blockers), dyssynchrony, and myocardial ischaemia or infarction. E_{es} is a relatively load-independent measure of LV contractility.[2,7,10,11]

Because ESPVR is a regression between multiple correlated V_{es} and P_{es} points, the impact of an intervention must simultaneously consider changes in E_{es} and V_0. Increased contractility occurs when changes in E_{es} and V_0 result in a leftward and/or upward ESPVR shift. Another index, V_{100}, is the ESPVR-extrapolated (or interpolated) volume at 100 mmHg. V_{100} typically lies within the physiological range of PV values (*Figure 2A*). High V_{100} reflects decreased contractility and *vice versa*.[11]

End-diastolic pressure–volume relationships

In contrast to ESPVR, the EDPVR is non-linear (*Figure 3A*). The EDPVR reflects the passive mechanical properties of the LV chamber, when all actin–myosin bonds are uncoupled. Accordingly, the EDPVR is determined by the size, orientation and mass of myocytes, and the extracellular matrix. Fibrosis, ischaemia, oedema, myocyte remodelling, and hypertrophy affect the EDPVR. Its slope (dP/dV) indexes LV chamber stiffness, and is load-dependent. Compliance is the mathematical inverse of stiffness (i.e. dV/dP). The LV volume at 30 mmHg on the EDPVR (V_{30}) reflects compliance and would suggest *remodelling* (rightward shift of the EDPVR) or diastolic dysfunction (leftward shift of the EDPVR). V_{30} increases in HF with reduced EF (HFrEF) and decreases in restrictive and hypertrophic cardiomyopathies.[11]

Ventricular performance is also highly influenced by the rate of relaxation (or lusitropy) (*Figure 3B*). The rate of pressure decay during isovolumetric relaxation is characterized by an exponential time constant of decay (τ), or the time for pressure to fall by 50% ($t_{1/2}$), reflecting the average rate of cross-bridge uncoupling within the myocytes. A normal value of τ is ~20–30 ms. Impaired relaxation (e.g. LV hypertrophy, ischaemia) prolongs τ (e.g. 70–100 ms) and will affect LV diastolic filling especially at higher heart rates (*Figure 3B*). The maximal rate of pressure fall during relaxation ($-dP/dt_{max}$) is also used, but is highly load-dependent.[12]

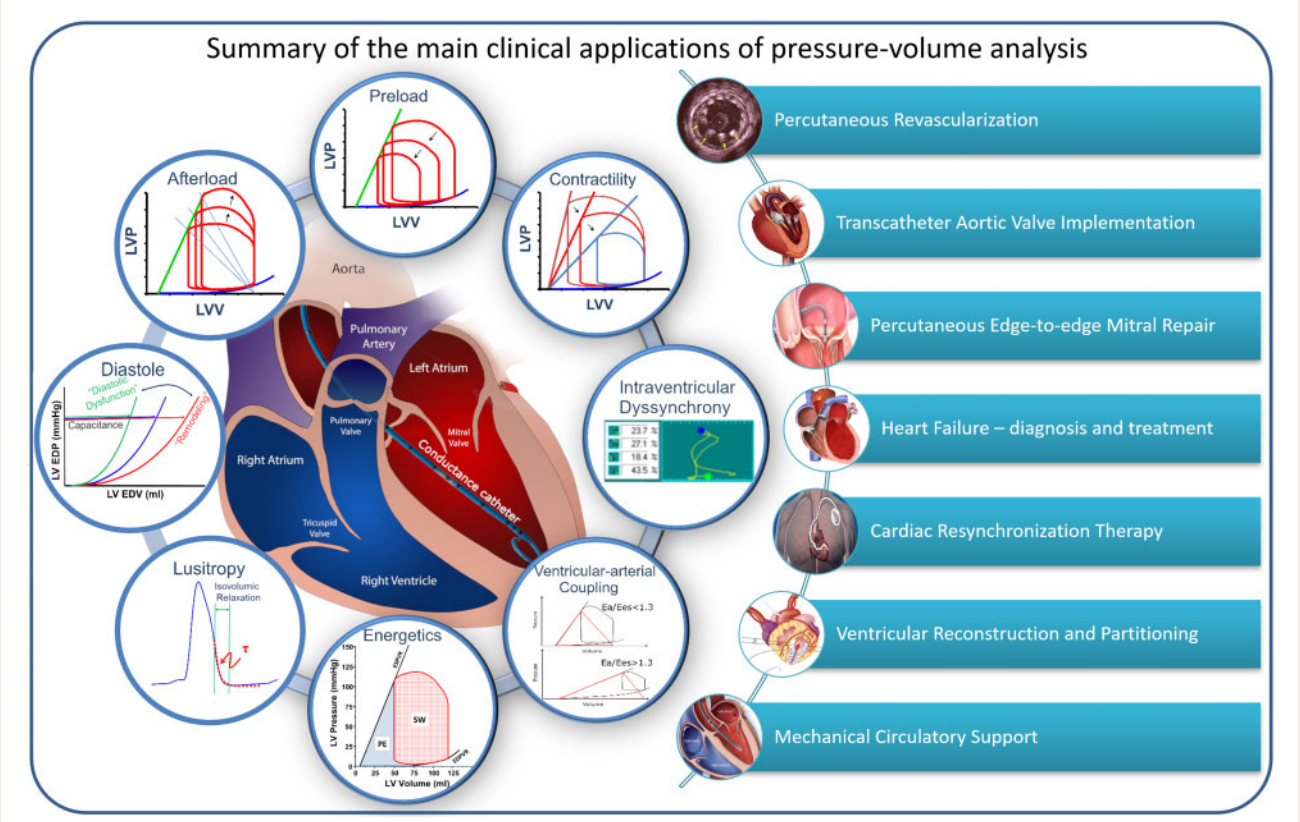

Take home figure Fundamental concepts of pressure–volume analysis and an overview of (potential) clinical applications.

Early diastolic suction

Under conditions of restrictive inflow elastic recoil may continue after the isovolumetric relaxation and mitral valve opening and cause a further LV pressure decline despite volume increase. The diastolic portion of the PV loop can fall below the zero-pressure line (*Figure 3C*). This diastolic suction phenomenon may enhance filling in conditions such as mitral stenosis and fluid depletion, but is blunted in HFrEF and HFpEF when filling pressures are high and there is no limitation of flow from the atrium to the ventricle.[20]

Ventricular-arterial coupling

The effective arterial elastance (E_a) is the slope of the line connecting V_{ed} on the volume axis to the end-systolic PV point on the PV loop. Accordingly, E_a is the ratio between P_{es} and SV (*Figure 2A*) and is determined by total peripheral resistance and heart rate ($E_a \propto$ TPR·HR). The ratio between E_a and E_{es} represents an index of ventricular-arterial coupling (VAC). Under normal conditions, E_a/E_{es} varies around 0.6 in humans. Within this range, there is optimal matching of ventricular and vascular properties so that values of stroke work (SW) and overall metabolic efficiency are near optimum values. HFrEF increases E_a and decreases E_{es} so that the E_a/E_{es} increases, which reflects ventricular-arterial mismatching. In contrast, age and hypertension increase E_a and E_{es} resulting in a normal or slightly elevated E_a/E_{es}. Finally, exercise in healthy individuals elevates E_{es} but reduces E_a lowering E_a/E_{es}, and suggesting more efficient energy transfer from the LV to the periphery (SW).[2,8,17,21]

Myocardial energetics

The total LV mechanical energy per beat is indexed by the PV area (PVA), which is the sum of the SW (i.e. the area within the PV loop) and the residual potential energy (PE) stored in the myocardium at the end of contraction (*Figure 4A*). Clinically, SW is estimated by the product of SV and mean arterial pressure (MAP) during ejection (SW $\approx$ SV · MAP). Stroke work represents the energy required to propel blood across the vasculature. Potential energy is the remaining energy stored in the myofilaments at the end of systole that is not dissipated as external SW. The PVA correlates linearly with the myocardial oxygen consumption per beat (MVO_2) (*Figure 4B*). Total MVO_2 includes the basal metabolism, intracellular calcium cycling involving the sarcoplasmic reticulum (both independent of PVA) and cross-bridge cycling (directly proportional to PVA). Changes in ventricular contractility are generally due to changes in calcium cycling and cause concomitant changes in the MVO_2 axis intercept of the MVO_2–PVA relationship.[2]

When multiplied by HR, PVA represents total power output (i.e. PVA·HR). Total power output is useful in evaluating the effects of

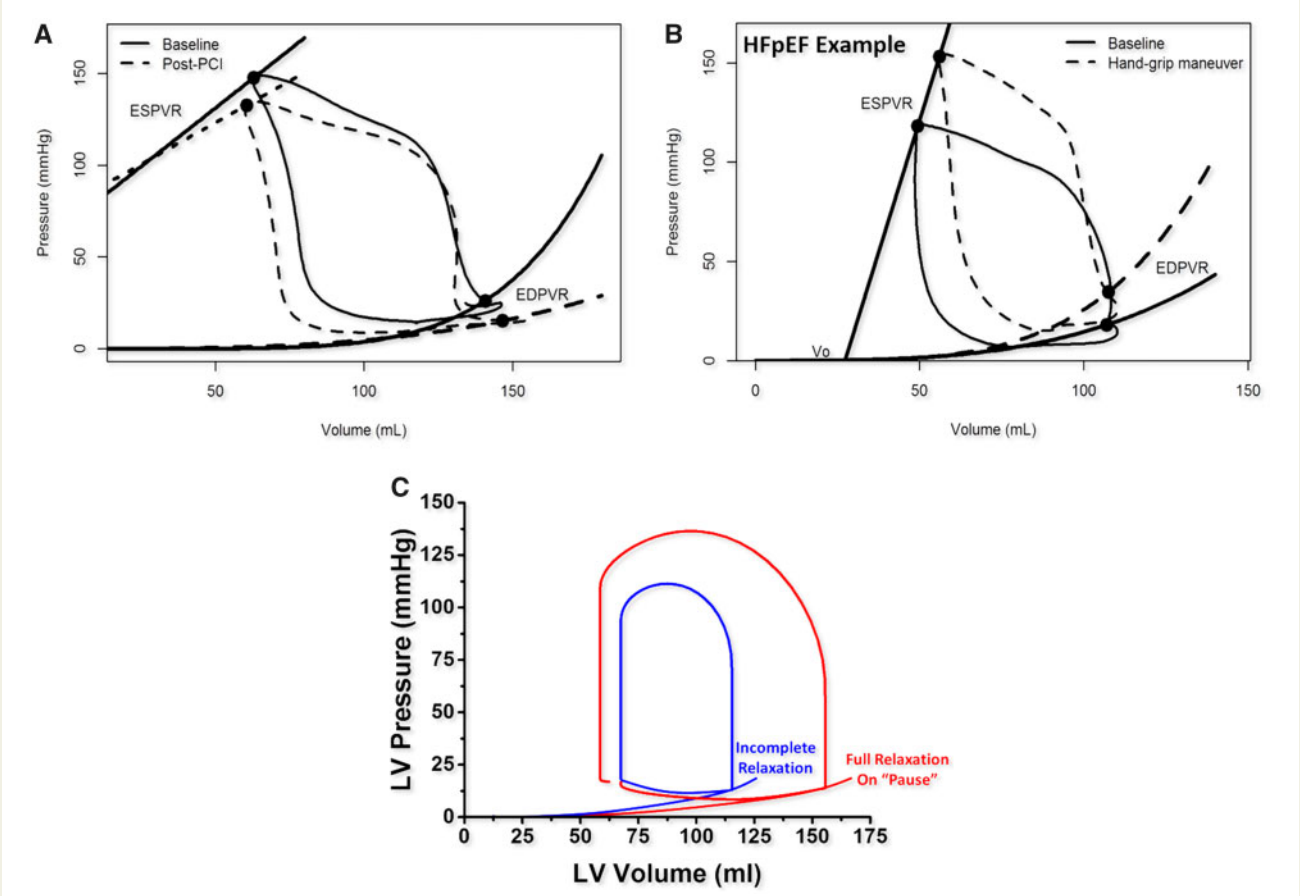

Figure 6 Effects of chronic ischaemia and incomplete relaxation on the pressure–volume loop. (*A*) Effect of percutaneous coronary revascularization with more vertical isovolumetric contraction and flatter end-diastolic pressure–volume relationship (dashed line). (*B*) Heart failure with preserved ejection fraction with increased P_{es}, elevated end-diastolic pressure–volume relationship and decreased stroke volume after handgrip manoeuvre (dashed line). (*C*) Incomplete relaxation (blue) unmasked by the occurrence of full relaxation during the refractory pause following an ectopic beat (red).

inotropes and different classes of mechanical circulatory support devices as these affect cardiac metabolism during ischaemia and cardiogenic shock.[22]

Intra-ventricular dyssynchrony

Segmental PV loops help evaluate dyssynchrony (*Figure 5*). When a segment is 'synchronous', the segmental PV loops are in phase with the global PV relationship. Dyssynchronous segmental PV loops appear distorted, progressing to a figure-of-eight and running out of phase in a counter-clockwise rotation. Segmental dyssynchrony is quantified by the percent of time a segment is moving in a direction opposite to the total volume change; total ventricular dyssynchrony is the average of segmental dyssynchrony of all segments. Dyssynchrony can be further quantified as the percentage of the energy mobilized by a non-dyssynchronic PV loop (cycle efficiency). Cycle efficiency decreases when more segmental PV loops have distorted shapes.[5,10,12,13,15]

Clinical applications

Left ventricular PV analysis in the catheterization laboratory provides important contributions to the understanding of the pathophysiology, diagnosis, and treatment of various conditions (*Take home figure*). Below we discuss salient findings in various cardiac conditions using real patient data and cardiovascular simulations.[18]

Myocardial ischaemia

In haemodynamically significant coronary stenosis, perfusion pressure falls and contractility decreases. Regional ischaemia induces focal hypo-contractility (hypo- or akinesia) and dyssynchrony that disturbs normal isovolumetric processes. Concomitantly, active relaxation (τ) is impaired. In the setting of prolonged τ, tachycardia leaves insufficient time between contractions for uncoupling of all actin–myosin bonds, a phenomenon called incomplete relaxation. This amplifies diastolic dysfunction and elevates the EDPVR. Higher end-diastolic pressures (P_{ed}) are required to maintain SV. Ischaemic

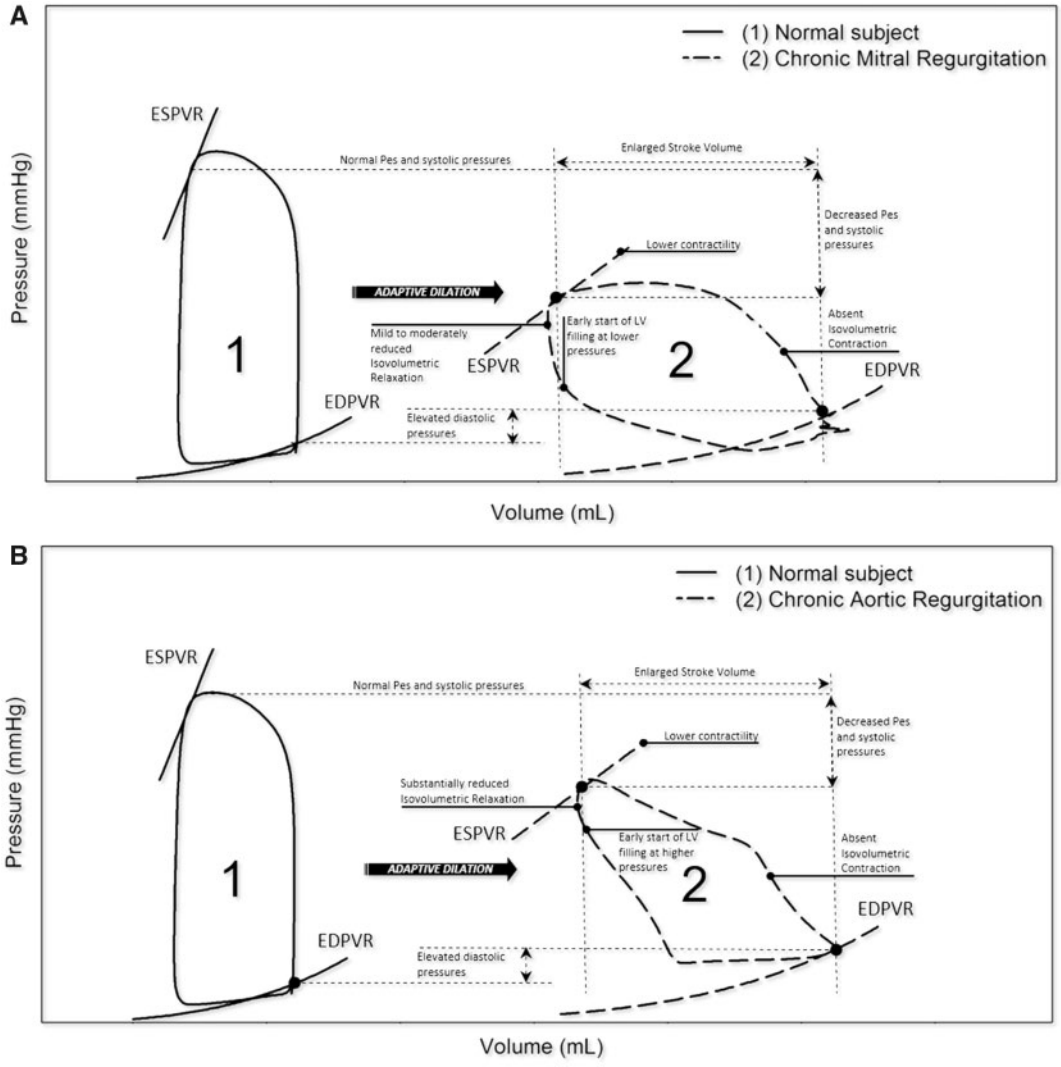

Figure 7 Pressure–volume loops in mitral and aortic regurgitation. (*A*) Chronic mitral regurgitation: right shifting with flatter end-systolic pressure–volume relationship, absent isovolumetric contraction and increased global stroke volume. (*B*) Chronic aortic regurgitation: right shifting with flatter end-systolic pressure–volume relationship and blunted isovolumetric phases (contraction and relaxation).

cardiomyopathy (*Figure 6A*) and exercise in HFpEF follow similar principles (*Figure 6B*). Incomplete relaxation can be distinguished from true shifts of the EDPVR in real time by observing changes in the diastolic portion of the PV loop during a pause when prolonged diastole allows for full relaxation (*Figure 6C*).[23–26]

The PV loop monitoring may provide sensitive real-time beat-to-beat assessment of the effects of myocardial ischaemia during high-risk percutaneous coronary interventions, especially when performed on proximal segments that serve perfusion to large downstream myocardial territories. Early detection of systolic and/or diastolic dysfunction would allow for timely adjustment of treatment strategies to prevent haemodynamic compromise and pulmonary oedema.[25,26]

Mitral and aortic regurgitation

Mitral and aortic regurgitation (MR and AR) demonstrate characteristic changes in the LV PV loop shape (*Figure 7*). Chronically, EDPVRs and PV loops shift rightwards (i.e. adaptive chamber dilatation or remodelling) reflecting fluid overload and increased LV P_{ed}.[27–29]

In MR (*Figure 8A*), the isovolumetric contraction is shortened and ejection starts earlier due to the regurgitant backflow. At end-systole, regurgitation can further reduce LV volume even after aortic valve closure, until LV pressure falls below the left atrial pressure. Conversely, in AR (*Figure 7B*), the diastolic aortic pressure is lower, which mitigates the isovolumetric contraction and favours premature ejection. The isovolumetric relaxation disappears due

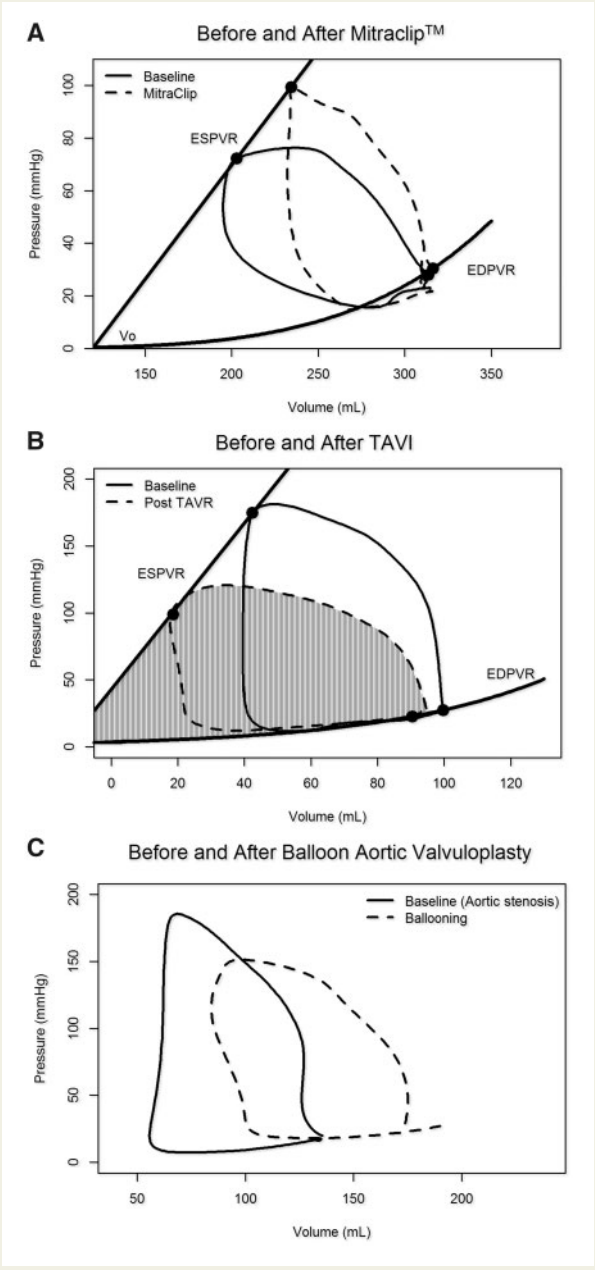

Figure 8 Pressure–volume loops with transcatheter valve interventions. (*A*) Edge-to-edge repair corrects mitral regurgitation partially restoring isovolumetric contraction and relaxation, increasing afterload and end-systolic volume while decreasing stroke volume. (*B*) Transcatheter aortic valve implantation (TAVI) reduces afterload, increases stroke volume and reduces the pressure–volume area (hatched area). (*C*) Balloon aortic valvuloplasty decreases afterload. Note the reduced isovolumetric phases and early diastolic filling that suggest aortic regurgitation (dashed line).

to the regurgitant flow through the incompetent aortic valve.[27,28,30]

In both MR and AR, total SV (loop width) equals the sum of the forward plus regurgitant volumes. Thus, global EF may not be reflective of LV contractility. ESPVR and E_{es} remain valid measures of contractility because both are relatively load independent.[30–33]

The PV loops provide immediate insights into the effects of mitral interventions such as edge-to-edge mitral repair. Changing PV loop morphology can help tailor positioning and/or determine number of clips to optimize a final result and help differentiate responders from non-responders. Responders may show acute increases in P_{es} and V_{es}, with concomitant reduction in global SV and global EF (*Figure 8A*). Reductions of EF would then reflect relative changes in afterload and should not be interpreted as reductions in ventricular contractility.[33,34]

Mitral and aortic stenosis

Mitral stenosis reduces LV preload and increases pulmonary venous pressures. The ESPVR and active relaxation (τ) are preserved. Early diastolic suction could theoretically occur in early diastole (*Figure 3C*).[35]

Aortic stenosis (AS) augments total LV afterload and elevates E_a/E_{es}. In this setting, E_a reflects the combination of arterial and valvular resistances and is generally markedly increased. Pressure rises sharply during systole to a domed-shaped PV loop. V_{ed} remains close to normal but V_{es} is commonly increased, reflecting reduced SV. After TAVI, LV peak pressure and V_{ed} decrease while SV (and EF) can increase in response to the decreased afterload (*Figures 8B* and *9*).[27] During TAVI or balloon aortic valvuloplasty, acute changes in PV loops may help reveal the occurrence and functional significance of newly induced AR (*Figures 8C* and *9*).

Heart failure

Left ventricular PV analysis can help define underlying pathology, monitor disease progression, and interventions in HF. In HFpEF, incomplete relaxation causes exercise intolerance, mostly during tachycardia. E_a and E_{es} increase proportionally and the ratio E_a/E_{es} remains stable. The PV loop comparisons at rest and exercise can help to diagnose HFpEF (*Figure 6B*). Of note, HFpEF is characterized by similar effects in the RV and LV and helps explain the rapid rise of both central venous and pulmonary capillary wedge pressures with exercise.[8,23,24,36–38]

In HFrEF, the ESPVR, EDPVR, and PV loops shift rightwards due to ventricular remodelling (*Figures 3A* and *10*). There are significant increases in E_a/E_{es} ratio (>1.2) indicating ventricular-vascular mismatching that persists with exercise.[39]

Intra-ventricular dyssynchrony and cardiac resynchronization therapy

Dyssynchrony is common in HF, particularly in HFrEF patients with left bundle branch block. Invasive PV analysis may visually confirm baseline dyssynchrony and help select the most effective pacing site during cardiac resynchronization therapy (CRT) by monitoring the restitution of synchronization. In parallel, SW and contractility should improve (*Figure 5*).[15,40–42]

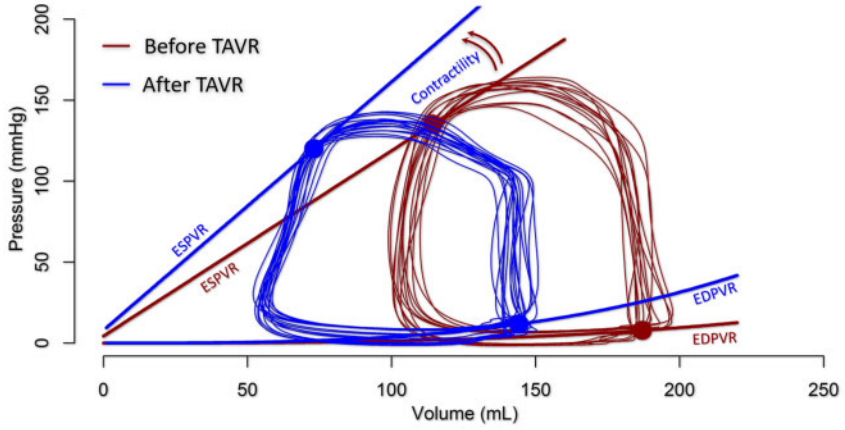

Figure 9 Pressure–volume relationship before (blue) and after (red) transcatheter aortic valve implantation in a patient with moderate aortic stenosis and depressed left ventricular systolic function. Contractility increases and the left ventricular is unloaded as characterized by a left shift of the pressure–volume loop.

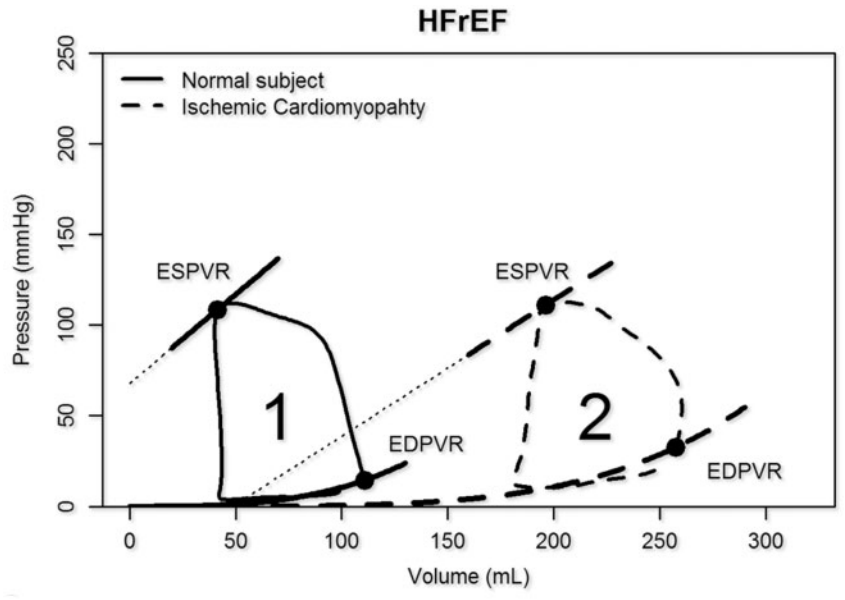

Figure 10 Heart failure with reduced ejection fraction (HFrEF). The pressure–volume diagram and the end-systolic pressure–volume relationship shift to the right while compliance is increased (remodelling).

Ventricular reconstruction and partitioning

The PV analysis revealed increased diastolic dysfunction after surgical ventricular reconstruction through resection of viable hypocontractile tissue in dilated cardiomyopathies because the EDPVR shifted more to the left than the ESPVR. Conversely, removal of post-infarct akinetic scar tissue created a more homogenous left shift of the EDPVR and ESPVR with no deleterious effect on overall LV function.[9,10,13,43–45]

Mechanical circulatory support

The intra-aortic balloon pump may provide some reductions in LV afterload and improve cardiac output and ventricular dyssynchrony in selected cases (*Figures 11* and *12A*).[12]

As more potent mechanical circulatory support emerged, PV analysis became the primary tool to assess their effect. The continuous flow axial percutaneous Impella (Abiomed Inc., Danvers, MA, USA) gradually shifts the PV loops to the left and downward (unloading) at higher flow states and making it triangular because isovolumetric contraction and relaxation fade (*Figure 12B*). In contrast, veno-arterial extracorporeal membrane oxygenation (VA-ECMO), pumps central venous blood to the arterial system via a membrane oxygenator. Veno-arterial extracorporeal membrane oxygenation unloads the right ventricle and improves peripheral oxygen delivery, but increases LV afterload shifting the PV loop toward higher end-diastolic volumes and pressures (*Figure 12C*). The increased afterload impedes aortic valve opening, promotes intra-ventricular dyssynchrony and reduces intrinsic SV. MVO_2 and pulmonary venous pressures increase. Left ventricular venting strategy with concomitant use of a percutaneous assist device can counteract these unfavourable VA-ECMO effects (*Figure 12D*).[22,46–48]

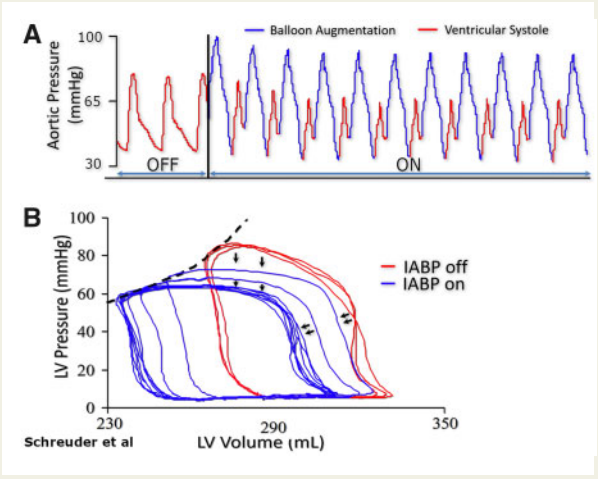

Figure 11 (*A*) Immediate effect of intra-aortic balloon pumping in a patient with 14% ejection fraction. (*B*) Pressure waveform showing characteristic diastolic augmentation when support is initiated. (*B*) Corresponding pressure–volume loops showing left shift with reduction in systolic pressures, and increased stroke volume.

Conclusion

Contemporary invasive PV analysis techniques provide real-time assessment of LV loading conditions, contractility, and indices of myocardial oxygen consumption. Further research is needed to determine whether such techniques can complement currently available measures of LV function and VAC to improve understanding of the pathophysiology and therapeutics of complex cardiac disease states in routine clinical practice.

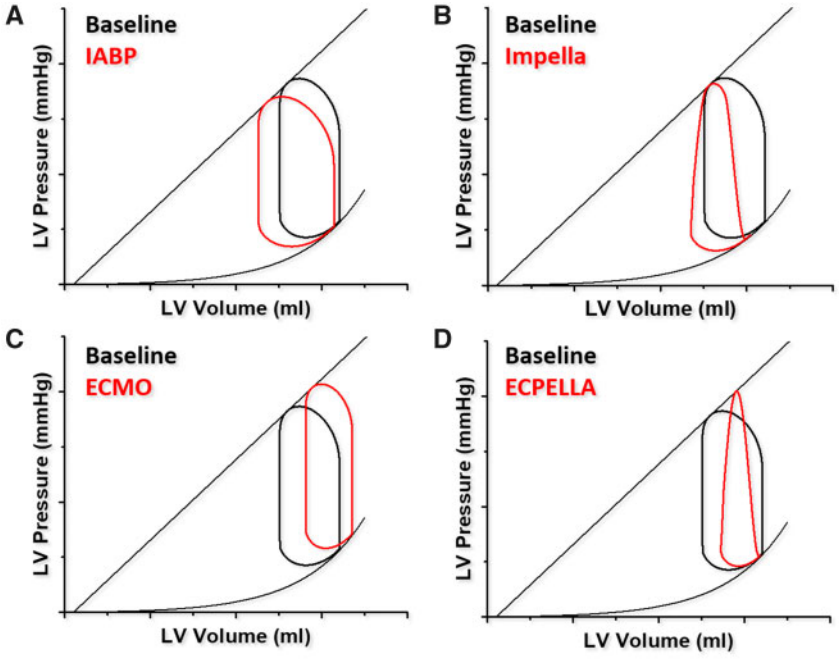

Figure 12 Pressure–volume effects of different mechanical circulatory support devices. (*A*) Intra-aortic balloon pump: left shifted and mildly increased stroke volume. (*B*) Impella: left shifted triangular loop with blunted isovolumetric phases. (*C*) Venous-arterial Extracorporeal Membrane Oxygenation (V-A ECMO): right shifted, increased afterload and reduced stroke volume. (*D*) Venous-arterial Extracorporeal Membrane Oxygenation vented by Impella (ECPELLA). Partial shift to the left with venting (in red) as compared to (*C*).

Conflict of interest: F.M. received research support and speaker honoraria from Medtronic and Recor, and is supported by Deutsche Hochdruckliga, Deutsche Gesellschaft für Kardiologie, and Deutsche Forschungsgemeinschaft (SFB TRR 219). D.B. is an author of the Harvi online simulator. N.V.M. is advisor to and has received research grants from Medtronic, Abbott, Boston Scientific, and PulseCath BV. The other authors report no conflicts.

References

1. Kuhtz-Buschbeck JP, Drake-Holland A, Noble MIM, Lohff B, Schaefer J. Rediscovery of Otto Frank's contribution to science. *J Mol Cell Cardiol* 2018;**119**:96–103.
2. Suga H. Ventricular energetics. *Physiol Rev* 1990;**70**:247–277.
3. Baan J, van der Velde ET, Steendijk P. Ventricular pressure-volume relations in vivo. *Eur Heart J* 1992;**13** Suppl E:2–6.
4. van der Velde ET, van Dijk AD, Steendijk P, Diethelm L, Chagas T, Lipton MJ, Glanz SA, Baan J. Left ventricular segmental volume by conductance catheter and Cine-CT. *Eur Heart J* 1992;**13** Suppl E:15–21.
5. Steendijk P, Tulner SA, Schreuder JJ, Bax JJ, van Erven L, van der Wall EE, Dion RA, Schalij MJ, Baan J. Quantification of left ventricular mechanical dyssynchrony by conductance catheter in heart failure patients. *Am J Physiol Heart Circ Physiol* 2004;**286**:H723–30.
6. Chen CH, Fetics B, Nevo E, Rochitte CE, Chiou KR, Ding PA, Kawaguchi M, Kass DA. Noninvasive single-beat determination of left ventricular end-systolic elastance in humans. *J Am Coll Cardiol* 2001;**38**:2028–2034.
7. Klotz S, Dickstein ML, Burkhoff D. A computational method of prediction of the end-diastolic pressure-volume relationship by single beat. *Nat Protoc* 2007;**2**:2152–2158.
8. Cohen-Solal A, Caviezel B, Himbert D, Gourgon R. Left ventricular-arterial coupling in systemic hypertension: analysis by means of arterial effective and left ventricular elastances. *J Hypertens* 1994;**12**:591–600.
9. Schreuder JJ, van der Veen FH, van der Velde ET, Delahaye F, Alfieri O, Jegaden O, Lorusso R, Jansen JR, Hoeksel SA, Finet G, Volterrani M, Kaulbach HG, Baan J, Wellens HJ. Left ventricular pressure-volume relationships before and after cardiomyoplasty in patients with heart failure. *Circulation* 1997;**96**:2978–2986.
10. Schreuder JJ, Steendijk P, van der Veen FH, Alfieri O, van der Nagel T, Lorusso R, van Dantzig JM, Prenger KB, Baan J, Wellens HJ, Batista RJ. Acute and short-term effects of partial left ventriculectomy in dilated cardiomyopathy: assessment by pressure-volume loops. *J Am Coll Cardiol* 2000;**36**:2104–2114.
11. Burkhoff D, Mirsky I, Suga H. Assessment of systolic and diastolic ventricular properties via pressure-volume analysis: a guide for clinical, translational, and basic researchers. *Am J Physiol Heart Circ Physiol* 2005;**289**:H501–12.
12. Schreuder JJ, Maisano F, Donelli A, Jansen JR, Hanlon P, Bovelander J, Alfieri O. Beat-to-beat effects of intraaortic balloon pump timing on left ventricular performance in patients with low ejection fraction. *Ann Thorac Surg* 2005;**79**:872–880.
13. Schreuder JJ, Castiglioni A, Maisano F, Steendijk P, Donelli A, Baan J, Alfieri O. Acute decrease of left ventricular mechanical dyssynchrony and improvement of contractile state and energy efficiency after left ventricular restoration. *J Thorac Cardiovasc Surg* 2005;**129**:138–145.
14. Schreuder JJ, Castiglioni A, Donelli A, Maisano F, Jansen JR, Hanania R, Hanlon P, Bovelander J, Alfieri O. Automatic intraaortic balloon pump timing using an intra-beat dicrotic notch prediction algorithm. *Ann Thorac Surg* 2005;**79**:1017–1022. discussion 1022.
15. de Roest GJ, Allaart CP, Kleijn SA, Delnoy PP, Wu L, Hendriks ML, Bronzwaer JG, van Rossum AC, de Cock CC. Prediction of long-term outcome of cardiac resynchronization therapy by acute pressure-volume loop measurements. *Eur J Heart Fail* 2013;**15**:299–307.
16. Burkhoff D, Sayer G, Doshi D, Uriel N. Hemodynamics of mechanical circulatory support. *J Am Coll Cardiol* 2015;**66**:2663–2674.
17. Chen CH, Nakayama M, Nevo E, Fetics BJ, Maughan WL, Kass DA. Coupled systolic-ventricular and vascular stiffening with age: implications for pressure regulation and cardiac reserve in the elderly. *J Am Coll Cardiol* 1998;**32**:1221–1227.
18. Burkhoff D, Dickstein ML, Schleicher T, Harvi—Online.https://harvi.online (1 December 2018).
19. Burkhoff D, van der Velde E, Kass D, Baan J, Maughan WL, Sagawa K. Accuracy of volume measurement by conductance catheter in isolated, ejecting canine hearts. *Circulation* 1985;**72**:440–447.
20. Little WC. Diastolic dysfunction beyond distensibility: adverse effects of ventricular dilatation. *Circulation* 2005;**112**:2888–2890.
21. De Tombe PP, Jones S, Burkhoff D, Hunter WC, Kass DA. Ventricular stroke work and efficiency both remain nearly optimal despite altered vascular loading. *Am J Physiol* 1993;**264**:H1817–24.
22. Burkhoff D, Naidu SS. The science behind percutaneous hemodynamic support: a review and comparison of support strategies. *Catheter Cardiovasc Interv* 2012;**80**:816–829.
23. Westermann D, Kasner M, Steendijk P, Spillmann F, Riad A, Weitmann K, Hoffmann W, Poller W, Pauschinger M, Schultheiss HP, Tschöpe C. Role of left ventricular stiffness in heart failure with normal ejection fraction. *Circulation* 2008;**117**:2051–2060.
24. Hay I, Rich J, Ferber P, Burkhoff D, Maurer MS. Role of impaired myocardial relaxation in the production of elevated left ventricular filling pressure. *Am J Physiol Heart Circ Physiol* 2005;**288**:H1203–8.
25. Hoole SP, Heck PM, White PA, Read PA, Khan SN, West NE, O'Sullivan M, Dutka DP. Stunning and cumulative left ventricular dysfunction occurs late after coronary balloon occlusion in humans insights from simultaneous coronary and left ventricular hemodynamic assessment. *JACC Cardiovasc Interv* 2010;**3**:412–418.
26. Ladwiniec A, White PA, Nijjer SS, O'Sullivan M, West NEJ, Davies JE, Hoole SP. Diastolic backward-traveling decompression (suction) wave correlates with simultaneously acquired indices of diastolic function and is reduced in left ventricular stunning. *Circ Cardiovasc Interv* 2016;**9**:
27. Bunnell IL, Grant C, Greene DG. Left ventricular function derived from the pressure-volume diagram. *Am J Med* 1965;**39**:881–894.
28. Regeer MV, Versteegh MI, Ajmone Marsan N, Schalij MJ, Klautz RJ, Bax JJ, Delgado V. Left ventricular reverse remodeling after aortic valve surgery for acute versus chronic aortic regurgitation. *Echocardiography* 2016;**33**:1458–1464.
29. Wisenbaugh T, Spann JF, Carabello BA. Differences in myocardial performance and load between patients with similar amounts of chronic aortic versus chronic mitral regurgitation. *J Am Coll Cardiol* 1984;**3**:916–923.
30. Gaasch WH, Meyer TE. Left ventricular response to mitral regurgitation: implications for management. *Circulation* 2008;**118**:2298–2303.
31. Pibarot P, Burkhoff D. Post-TAVR heart failure. *Structural Heart* 2018;**2**:286–290.
32. Dupuis M, Mahjoub H, Clavel MA, Côté N, Toubal O, Tastet L, Dumesnil JG, O'Connor K, Dahou A, Thébault C, Bélanger C, Beaudoin J, Arsenault M, Bernier M, Pibarot P. Forward left ventricular ejection fraction: a simple risk marker in patients with primary mitral regurgitation. *J Am Heart Assoc* 2017;**6**:
33. Schrage B, Kalbacher D, Schwarzl M, Rübsamen N, Waldeyer C, Becher PM, Tigges E, Burkhoff D, Blankenberg S, Lubos E, Schäfer U, Westermann D. Distinct hemodynamic changes after interventional mitral valve edge-to-edge repair in different phenotypes of heart failure: an integrated hemodynamic analysis. *J Am Heart Assoc* 2018;**7**:
34. Gaemperli O, Biaggi P, Gugelmann R, Osranek M, Schreuder JJ, Bühler I, Sürder D, Lüscher TF, Felix C, Bettex D, Grünenfelder J, Corti R. Real-time left ventricular pressure-volume loops during percutaneous mitral valve repair with the MitraClip system. *Circulation* 2013;**127**:1018–1027.
35. Liu CP, Ting CT, Yang TM, Chen JW, Chang MS, Maughan WL, Lawrence W, Kass DA. Reduced left ventricular compliance in human mitral stenosis. Role of reversible internal constraint. *Circulation* 1992;**85**:1447–1456.
36. Borlaug BA, Kass DA. Invasive hemodynamic assessment in heart failure. *Cardiol Clin* 2011;**29**:269–280.
37. Kawaguchi M, Hay I, Fetics B, Kass DA. Combined ventricular systolic and arterial stiffening in patients with heart failure and preserved ejection fraction: implications for systolic and diastolic reserve limitations. *Circulation* 2003;**107**:714–720.
38. Penicka M, Bartunek J, Trakalova H, Hrabakova H, Maruskova M, Karasek J, Kocka V. Heart failure with preserved ejection fraction in outpatients with unexplained dyspnea: a pressure-volume loop analysis. *J Am Coll Cardiol* 2010;**55**:1701–1710.
39. Asanoi H, Sasayama S, Kameyama T. Ventriculoarterial coupling in normal and failing heart in humans. *Circ Res* 1989;**65**:483–493.
40. Brutsaert DL. Nonuniformity: a physiologic modulator of contraction and relaxation of the normal heart. *J Am Coll Cardiol* 1987;**9**:341–348.
41. Lieberman R, Padeletti L, Schreuder J, Jackson K, Michelucci A, Colella A, Eastman W, Valsecchi S, Hettrick DA. Ventricular pacing lead location alters systemic hemodynamics and left ventricular function in patients with and without reduced ejection fraction. *J Am Coll Cardiol* 2006;**48**:1634–1641.
42. Daubert C, Behar N, Martins RP, Mabo P, Leclercq C. Avoiding non-responders to cardiac resynchronization therapy: a practical guide. *Eur Heart J* 2017;**38**:1463–1472.
43. Schreuder JJ, van der Veen FH, van der Velde ET, Delahaye F, Alfieri O, Jegaden O, Lorusso R, Jansen JR, van Ommen V, Finet G. Beat-to-beat analysis of left ventricular pressure-volume relation and stroke volume by conductance catheter and aortic Modelflow in cardiomyoplasty patients. *Circulation* 1995;**91**:2010–2017.
44. Burkhoff D, Wechsler AS. Surgical ventricular remodeling: a balancing act on systolic and diastolic properties. *J Thorac Cardiovasc Surg* 2006;**132**:459–463.
45. Artrip JH, Oz MC, Burkhoff D. Left ventricular volume reduction surgery for heart failure: a physiologic perspective. *J Thorac Cardiovasc Surg* 2001;**122**:775–782.
46. Neumann FJ, Sousa-Uva M, Ahlsson A, Alfonso F, Banning AP, Benedetto U, Byrne RA, Collet JP, Falk V, Head SJ, Jüni P, Kastrati A, Koller A, Kristensen SD, Niebauer J, Richter DJ, Seferovic PM, Sibbing D, Stefanini GG, Windecker S,

Yadav R, Zembala MO; ESC Scientific Document Group. ESC/EACTS Guidelines on myocardial revascularization. *Eur Heart J* 2019;**40**:87–165.
47. den Uil CA, Dos Reis Miranda D, Van Mieghem NM, Jewbali LS. A Niche indication for intra-aortic balloon pump counterpulsation: aortic valve opening in a surgically vented left ventricle on venoarterial ECMO. *JACC Cardiovasc Interv* 2017;**10**:e133–e134.
48. Ponikowski P, Voors AA, Anker SD, Bueno H, Cleland JGF, Coats AJS, Falk V, González-Juanatey JR, Harjola VP, Jankowska EA, Jessup M, Linde C, Nihoyannopoulos P, Parissis JT, Pieske B, Riley JP, Rosano GMC, Ruilope LM, Ruschitzka F, Rutten FH, van der Meer P, Group E. 2016 ESC Guidelines for the diagnosis and treatment of acute and chronic heart failure: the Task Force for the diagnosis and treatment of acute and chronic heart failure of the European Society of Cardiology (ESC)Developed with the special contribution of the Heart Failure Association (HFA) of the ESC. *Eur Heart J* 2016;**37**:2129–2200.